A Mathematical Model for Competition Between Local and Invasive Fish in Lake Poso, Indonesia

Tokonyai Tawanda Jonathan Rabvemhiri[1], **Hajar**[3], **Juni Wijayanti Puspita**[3] **Dipo Aldila**[1,2,*]

[1]Department of Mathematics, Faculty of Mathematics and Natural Sciences, Universitas Indonesia,
Depok 16424, Indonesia
[2]Innovative Mathematics and Predictive Analytics for Complex System and Technology Laboratory (IMPACT Lab),
Universitas Indonesia, Depok 16424, Indonesia
[3]Mathematics Study Program, Tadulako University, Palu 94118, Indonesia

*Email: aldiladipo@sci.ui.ac.id

Abstract

The introduction of *Nile Tilapia* into Lake Poso has created both ecological and economic challenges, particularly in its interaction with the endemic species *Oryzias nigrimas*. To understand the potential long-term impacts of this competition and the community's economic use of *Nile Tilapia*, we introduced a novel mathematical model describing their population dynamics. The model is formulated as a four-dimension ordinary differential equations and analyzed for the positivity of solutions, existence and local stability of equilibrium points, and the influence of harvesting strategies. Numerical simulations, including bifurcation and time-series analyses, are conducted to assess the effects of constant and periodic harvesting of *Nile Tilapia*. The findings suggest that periodic harvesting can play a significant role in maintaining population balance and mitigating the ecological pressure on *Oryzias nigrimas*, offering insights for sustainable management of invasive fish in Lake Poso.

Keywords: *Nile Tilapia, Oryzias nigrimas, Lake Poso, mathematical model, harvesting, bifurcation*

2020 MSC classification number: 92D40, 92D25, 92B05

1. INTRODUCTION

Lake Poso is one of the ancient lakes in Central Sulawesi, Indonesia, with high ecological value and serves as a key habitat supporting a wide range of endemic species. The lake is recognized as one of the freshwater fish biodiversity hotspots in Sulawesi, with a total of 30 recorded species, most of which are harvested for consumption or collected as ornamental fish. This uniqueness is further reflected by the presence of 15 endemic species associated with three major habitats in Sulawesi — Lindu, Poso, and Tiu — consisting of four species of Adrianichthys, six of Oryzias, two of Mugilogobius, and three of Nomorhamphus [1]. Among these endemic fishes, one of the most emblematic species is Oryzias nigrimas, a ricefish exclusively distributed in Lake Poso [2]. Phylogenetic analyses further show that the genus Oryzias comprises three major clades — latipes, javanicus, and celebensis — with *Oryzas Nigrimas* (Kottelat, 1990) belonging to the celebensis clade and being endemic to Central Sulawesi [3].

Despite its high levels of biodiversity, the Lake Poso ecosystem is currently experiencing substantial ecological pressure, particularly from introduced fish species that compete with endemic fishes, monopolize habitat space, and reduce their access to food resources and refugia [4]. Among these introduced species, *Nile Tilapia* (Oreochromis niloticus) has become one of the most ecologically impactful invaders, posing a direct threat to *Oryzas Nigrimas* through resource competition and habitat takeover. Studies conducted in tropical shallow lakes rich in macrophytes have shown that juvenile *Nile Tilapia* may facilitate macrophyte growth by consuming periphyton and seston—both of which are major food sources for *Oryzas Nigrimas*—whereas adult individuals have the potential to suppress macrophyte growth. Consequently, *Nile Tilapia* can alter the aquatic environment and cause habitat degradation, which risks reducing the survival of *Oryzas Nigrimas* populations [5].

---

*Corresponding Author

Received November 10^{th}, 2025, Revised February 15^{th}, 2026, Accepted for publication April 16^{th}, 2026. e-ISSN: 2549-2896, DOI:10.5614/cbms.2026.9.1.6

Various studies have used mathematical modeling approaches to understand ecosystem dynamics and interspecies interactions within biological communities [6, 7, 8, 9, 10]. Tabornal et al. [11] developed a Hill-type model that highlights how competition and cooperation influence species survival, including the possibilities of coexistence, exclusion, or extinction, while Gutnik et al. [12] investigated two-species competition for limited resources by integrating the principles of Gause, Tilman, and Michaelis–Menten, demonstrating that resource capacity dictates coexistence and survival. Lu et al. [13] further incorporated double time delays into a two-species competition model and revealed that such delays can significantly alter system stability. Other studies have focused on the role of external factors in regulating ecological balance. For example, Shukla et al. [14] examined the effects of toxic emissions in polluted environments on two-species competition, whereas Omaiye [15] emphasized the importance of abiotic and biotic drivers in shaping multispecies community structure. Chen et al. [16] and chen et al. [17] expanded classical ecological models by incorporating allelopathy, fear effects, and Allee effects, all of which were shown to influence extinction dynamics and coexistence, while Hu et al. [18] introduced seasonal perturbation into a three-species impulsive system and demonstrated that environmental variability can generate periodic fluctuations in population. From the perspective of invasive–endemic interactions, Lou et al. [19] analyzed predator-mediated apparent competition between endemic prey and invasive species, indicating that predators can either exacerbate or stabilize population imbalances, and Leticia and Olekal [20] explored dynamic behavior of two competing plant species as an important analogue for aquatic ecosystems. Collectively, these studies illustrate that mathematical models are essential for explaining coexistence, competition, and complex ecological impacts in multispecies systems—including in the case of Lake Poso, where endemic species such as *Oryzas Nigrimas* are increasingly threatened by introduced fish such as *Nile Tilapia*.

Based on the above description, we observe two key points. First, the interaction between *Oryzias nigrimas* and *Nile Tilapia* in Lake Poso requires a multidisciplinary approach to better understand the potential future impacts of their competition, particularly concerning the introduction of *Nile Tilapia* and the community's attempt to gain economic benefits from it. Second, no mathematical study has yet examined the interaction between these two species in Lake Poso. Therefore, in this article, we propose a novel mathematical model to investigate the interaction between *Oryzias nigrimas* and *Nile Tilapia* in Lake Poso and to further analyze the effects of specific harvesting strategies on *Nile Tilapia*. The proposed model is formulated as a system of ordinary differential equations and analyzed in terms of the positivity of its solutions, the existence and stability of equilibrium points, and numerical experiments on the effects of constant and periodic harvesting of *Nile Tilapia*.

The paper is organized as follows. In Section 2, we introduce our model, demonstrate the positivity criteria, and present its nondimensionalization. In Section 3, we analyze the model in terms of the existence and local stability of the equilibrium points. Section 4 is dedicated to numerical experiments, including the bifurcation diagram, autonomous and non-autonomous simulations, specifically focusing on the impact of periodic harvesting on *Nile Tilapia*. Finally, some conclusions are provided in Section 5.

2. MODEL FORMULATION AND PRELIMINARY ANALYSIS

2.1. Model Formulation

The presence of *Nile Tilapia* in Lake Poso Poso poses a potential threat to the survival of the endemic fish, *Oryzias nigrimas*, because the food sources normally consumed by *Oryzas Nigrimas* are also consumed by this introduced species. The foraging activities of *Nile Tilapia* can alter habitat structure, thereby affecting resource availability and ecological conditions for the endemic populations. *Oryzas Nigrimas* exhibits an omnivorous feeding pattern, with phytoplankton as its primary food source, supplemented by diatoms, shrimp larvae, and zooplankton [21]. Previous studies reported that juvenile *Nile Tilapia* may facilitate macrophyte growth that is also utilized by *Oryzas Nigrimas*, whereas adult individuals tend to suppress macrophyte development and aggressively interfere with *Oryzas Nigrimas*, thereby altering aquatic dynamics in Lake Poso and reducing the survival prospects of this endemic species [5, 22, 21].

Let us assume that *Oryzas Nigrimas* is denoted by X, while *Nile Tilapia* is denoted by Y. Each population is divided into juvenile and adult populations. Hence, the juvenile and adult populations of *Oryzas Nigrimas* are denoted by X_1 and X_2, respectively. Similarly, the juvenile and adult *Nile Tilapia* are denoted by Y_1 and Y_2, respectively. Each population is assumed to grow following a logistic equation model with specific carrying capacities K and M for *Oryzas Nigrimas* and *Nile Tilapia*, respectively.

We assume that *Oryzas Nigrimas* grows with an intrinsic growth rate of $\bar{r}$, with the transition from juvenile to adult denoted by $\bar{\alpha}$. Each subpopulation of *Oryzas Nigrimas* can engage in competitive contact with *Nile Tilapia*, which reduces the population of *Oryzas Nigrimas* with specific contact rates $\bar{\beta}$ and $\bar{\eta}$ for the juvenile and adult populations, respectively. The interference interaction between two species is modeled using mass action function in our model, representing density-dependent encounters between species. This formulation assumes that the frequency of ecological interaction is proportional to the product of the two species, which is reasonable under homogeneous spatial mixing and overlapping habitat distribution. With the natural death rate of the adult population given by $\bar{\epsilon}$, the model for *Oryzas Nigrimas* is given by:

$$\frac{dX_1}{dt} = \bar{r}X_2\left(1-\frac{X_1+X_2}{K}\right) - \bar{\alpha}X_1 - \bar{\beta}X_1Y_2, \tag{1a}$$

$$\frac{dX_2}{dt} = \bar{\alpha}X_1 - \bar{\epsilon}X_2 - \bar{\eta}X_2Y_2, \tag{1b}$$

with each parameter assumed to be positive.

On the other hand, we assume that the *Nile Tilapia* in Lake Poso is not a newly introduced species. This fish has already existed in Lake Poso for many decades and has become well integrated into the ecosystem. Therefore, instead of modeling it as a species introduced through human intervention, we use a logistic model to describe the growth of this population, with its intrinsic growth rate denoted by $\bar{s}$. We assume that juvenile *Nile Tilapia* grow into adults at a constant rate $\bar{\gamma}$, and the adult population has a natural death rate of $\bar{\delta}$. It is further assumed that only the adult *Nile Tilapia* are aggressive toward both juvenile and adult populations of *Oryzas Nigrimas*. In contrast, *Oryzas Nigrimas* are considered a *Relatively non-aggressive* compared to *Nile Tilapia*, or at least we may assume it negligible interference compared to tilapia. This assumption is biologically motivated by the different body size between these two species, where adult *Nile Tilapia* are known to exhibit territorial behaviour ad stronger competition for space and resource. In our model, the term "aggressiveness" represent asymetric interference competition, rather than a general behavioral claim. Therefore, the assumption of realtively non-aggressive of *Oryzias Nigrimas* refer to it weaker interference competition, not the absence of ecological interaction between two species. Consequently, only the adult *Nile Tilapia* population can be reduced due to interspecific competition. Assuming that contact with adult *Oryzas Nigrimas* may result in the death of *Nile Tilapia* at a contact rate $\bar{\xi}$, and with human harvesting occurring at rate $\bar{u}$, the model is given by:

$$\frac{dY_1}{dt} = \bar{s}Y_2\left(1-\frac{Y_1+Y_2}{M}\right) - \bar{\gamma}Y_1, \tag{2a}$$

$$\frac{dY_2}{dt} = \bar{\gamma}Y_1 - \bar{\delta}Y_2 - \bar{\xi}X_2Y_2 - \bar{u}Y_2, \tag{2b}$$

with all parameters assumed to be non-negative.

With the model description given previously, the complete mathematical model for the interaction between *Oryzas Nigrimas* and *Nile Tilapia* is governed by the following system of nonlinear ordinary differential equations:

$$\frac{dX_1}{dt} = \bar{r}X_2\left(1-\frac{X_1+X_2}{K}\right) - \bar{\alpha}X_1 - \bar{\beta}X_1Y_2, \tag{3a}$$

$$\frac{dX_2}{dt} = \bar{\alpha}X_1 - \bar{\epsilon}X_2 - \bar{\eta}X_2Y_2, \tag{3b}$$

$$\frac{dY_1}{dt} = \bar{s}Y_2\left(1-\frac{Y_1+Y_2}{M}\right) - \bar{\gamma}Y_1, \tag{3c}$$

$$\frac{dY_2}{dt} = \bar{\gamma}Y_1 - \bar{\delta}Y_2 - \bar{\xi}X_2Y_2 - \bar{u}Y_2, \tag{3d}$$

completed with a non-negative initial conditions:

$$X_1(0) \geq 0, X_2(0) \geq 0, Y_1(0) \geq 0, Y_2(0) \geq 0.$$

furthermore, we have $X_1(0)+X_2(0) < K$, and $Y_1(0)+Y_2(0) \leq M$. It is important to note that in our model, the logistic growth terms represent intra-specific density dependence due to environmental limitations such as habitat capacity and spawning space in Lake Poso. The carrying capacity parameters are assumed species-specific (denoted by K and M), reflecting ecological constraints acting independently on each population. Interspecific ecological interaction is incorporated separately through the interference and contact terms (denoted by parameter $\bar{\beta}, \bar{\eta}$, and $\bar{\xi}$) rather than through a shared carrying capacity formulation. Furthermore, we assume that although *Nile Tilapia* is an invasive fish, it already "fully integrated" in Lake Poso. The term "fully integrated" here refers to the establishment of a self-sustaining and reproductively viable population within the ecosystem. It does not imply the absence of density-dependent regulation.

2.2. Well-Posedness of the Model

In this section, we establish the well-posedness of the model (3).

Theorem 2.1. *For positive initial conditions, every solution of model (3) remains positive for all* $t > 0$.

Proof: From Equation (3a) with its initial conditions, we obtain

$$\frac{dX_1}{X_1} = \left(\bar{r}\frac{X_2}{X_1}\left(1 - \frac{X_1 + X_2}{K}\right) - \bar{\alpha} - \bar{\beta}Y_2\right)dt.$$

By integrating the equation above within $[0, t]$,

$$X_1(t) = X_1(0)\exp\left(\int_0^t \left[\bar{r}\frac{X_2}{X_1}\left(1 - \frac{X_1 + X_2}{K}\right) - \bar{\alpha} - \bar{\beta}Y_2\right]ds\right) > 0.$$

Similarly, it can be shown that

$$\begin{aligned} X_2(t) &= X_2(0)\exp\left(\int_0^t \left[\bar{\alpha}\frac{X_1}{X_2} - \bar{\epsilon} - \bar{\eta}Y_2\right]ds\right) > 0, \\ Y_1(t) &= Y_1(0)\exp\left(\int_0^t \left[\bar{s}\frac{Y_2}{Y_1}\left(1 - \frac{Y_1 + Y_2}{M}\right) - \bar{\gamma}\right]ds\right) > 0, \\ Y_2(t) &= Y_2(0)\exp\left(\int_0^t \left[\bar{\gamma}\frac{Y_1}{Y_2} - \bar{\delta} - \bar{\xi}X_2 - \bar{u}\right]ds\right) > 0. \end{aligned}$$

Thus, according to [23], the solution of model (3) remains positive for all $t > 0$. ■

Theorem 2.2. *All solutions of the model (3) in* $\mathbb{R}^4_+$ *are uniformly bounded.*

Proof: By adding Equations (3a) and (3b) , we obtain

$$\begin{aligned} \frac{d(X_1 + X_2)}{dt} &= \bar{r}X_2\left(1 - \frac{X_1 + X_2}{K}\right) - \bar{\beta}X_1Y_2 - \bar{\epsilon}X_2 - \bar{\eta}X_2Y_2 \\ &< (\bar{r} - \bar{\epsilon})X_2 - \frac{\bar{r}X_2^2}{K}. \end{aligned}$$

For any positive constant φ, we have

$$\begin{aligned} \frac{d(X_1 + X_2)}{dt} + \varphi(X_1 + X_2) &< (\bar{r} - \bar{\epsilon})X_2 - \frac{\bar{r}X_2^2}{K} + \varphi(X_1 + X_2) \\ &= (\bar{r} - \bar{\epsilon} + \varphi)X_2 - \frac{\bar{r}X_2^2}{K} + \varphi X_1 \\ &= -\frac{\bar{r}}{K}\left[\left(X_2 - \frac{(\bar{r} - \bar{\epsilon} + \varphi)K}{2\bar{r}}\right)^2 - \left(\frac{(\bar{r} - \bar{\epsilon} + \varphi)K}{2\bar{r}}\right)^2\right] \\ &< \frac{(\bar{r} - \bar{\epsilon} + \varphi)^2K}{4\bar{r}}. \end{aligned}$$

Thus, $\frac{dX}{dt} + \varphi X < N$, where $N = \frac{(\bar{r} - \bar{\epsilon} + \varphi)^2K}{4\bar{r}}$ and $X = X_1 + X_2$. Following the differential inequality argument adopted by [24], it is easy to show that the solution of the above first order differential inequality satisfies $X(t) < \frac{N}{\varphi} + (X(0) - \frac{N}{\varphi})e^{-\varphi t}$. If $t \to \infty$, then $X(t) \to \frac{N}{\varphi}$. Consequently, X_1 and X_2 are bounded.

Similarly, from Equations (3c) and (3d), it can be shown that

$$\frac{d(Y_1+Y_2)}{dt}+\varphi(Y_1+Y_2) \quad < \quad (\bar{s}-\bar{\delta}-\bar{u}+\varphi)Y_2-\frac{\bar{s}Y_2^2}{M}+\varphi Y_1<\frac{(\bar{s}-\bar{\delta}-\bar{u}+\varphi)^2M}{4\bar{s}}.$$

Therefore, Y_1 and Y_2 are bounded, which completes the proof. ■

2.3. Non-dimensionalization of the Original Model

To simplify the model, we scale the variables with their respective carying capacity and the time is scaled to the transition rate $\bar{\alpha}$. Therefore, by assuming $x_1=\frac{X_1}{K}, x_2=\frac{X_2}{K}, y_1=\frac{Y_1}{M}, Y_2=\frac{Y_2}{M}, t=\frac{\tau}{\alpha}$ and

$$r=\frac{\bar{r}}{\bar{\alpha}},\quad s=\frac{\bar{s}}{\bar{\alpha}},\quad \beta=\frac{\bar{\beta}M}{\bar{\alpha}},\quad \eta=\frac{\bar{\eta}M}{\bar{\alpha}},\quad \epsilon=\frac{\bar{\epsilon}}{\bar{\alpha}},\quad \gamma=\frac{\bar{\gamma}}{\bar{\alpha}},\quad \delta=\frac{\bar{\delta}}{\bar{\alpha}},\quad \xi=\frac{\bar{\xi}K}{\bar{\alpha}},\quad u=\frac{\bar{u}}{\bar{\alpha}},$$

then our previous model in (3) now transforms into:

$$\frac{dx_1}{d\tau}=rx_2(1-x_1-x_2)-x_1-\beta x_1y_2, \tag{4a}$$

$$\frac{dx_2}{d\tau}=x_1-\varepsilon x_2-\eta x_2y_2, \tag{4b}$$

$$\frac{dy_1}{d\tau}=sy_2(1-y_1-y_2)-\gamma y_1, \tag{4c}$$

$$\frac{dy_2}{d\tau}=\gamma y_1-\delta y_2-\xi y_2x_2-uy_2. \tag{4d}$$

3. MODEL ANALYSIS

In this section, we analyze the existence and stability of each possible equilibrium point of system (4), both analytically and numerically. The equilibrium points are obtained by setting the right-hand side of system (4) equal to zero and solving it with respect to each variable. The equilibrium points are biologically meaningful only if they lie in the non-negative region of $\mathbb{R}^4_+$. For the stability analysis, we employ the linearization technique, where the Jacobian matrix of system (4) is given by:

$$\mathbf{J}=\begin{bmatrix} -\beta y_2-rx_2-1 & r\left(1-x_1-x_2\right)-rx_2 & 0 & -\beta x_1 \\ 1 & -\eta y_2-\epsilon & 0 & -\eta x_2 \\ 0 & 0 & -sy_2-\gamma & s\left(1-y_1-y_2\right)-sy_2 \\ 0 & -\xi y_2 & \gamma & -\xi x_2-\delta-u \end{bmatrix}. \tag{5}$$

3.1. Extinction of All Species

The first equilibrium is the extinction of both species from the ecosystem in Poso Lake, which is given by:

$$E_0=(x_1,x_2,y_1,y_2)=(0,0,0,0). \tag{6}$$

This equilibrium is always has a biological meaning without any condition. For the stability criteria, we evaluate $\mathbf{J}$ in Equation (5) in E_0, and we obtain:

$$\mathbf{J}(E_0)=\begin{pmatrix} -1 & r & 0 & 0 \\ 1 & -\epsilon & 0 & 0 \\ 0 & 0 & -\gamma & s \\ 0 & 0 & \gamma & -(\delta+u) \end{pmatrix}.$$

The characteristic polynomial of $\mathbf{J}(E_0)$ is given by:

$$P_1(\lambda)\ P_2(\lambda)=0,$$

where

$$\begin{aligned} P_1(\lambda) &= \lambda^2 + (1+\epsilon)\lambda + (\epsilon - r), \\ P_2(\lambda) &= \lambda^2 + (\gamma+\delta+u)\lambda + \gamma(\delta+u-s). \end{aligned}$$

It can be seen clearly that $P_1(\lambda)$ and $P_2(\lambda)$ will always have roots with negative real parts only if their zero-order coefficients of λ are positive, i.e., if and only if $R_1 = \dfrac{r}{\epsilon} < 1$ and $R_2 = \dfrac{s}{\delta+u} < 1$. This result is stated in the following theorem.

Theorem 3.1. *The equilibrium point E_0 of system (4) are locally asymptotically stable if and only if*

$$R_1 = \frac{r}{\epsilon} < 1 \quad \textit{and} \quad R_2 = \frac{s}{\delta+u} < 1.$$

Otherwise, if either $R_1 > 1$ or $R_2 > 1$, then E_0 becomes unstable.

From the expressions of R_1 and R_2, we can see that both thresholds play an important role in determining the stability of E_0. The quantities R_1 and R_2 can be interpreted as the minimum requirements for the persistence of each population. The condition $R_1 > 1$ indicates that the growth rate of *Oryzas Nigrimas* exceeds its natural death rate. On the other hand, $R_2 > 1$ implies that the growth rate of *Nile Tilapia* is greater than its total death rate, which consists of both the natural death rate and the harvesting rate.

3.2. Extinction of *Nile Tilapia*

The second equilibrium is given when the population of *Nile Tilapia* extinct from the ecosystem in Poso Lake. From direct calculation, this equilibrium is given by:

$$E_1 = (x_1, x_2, y_1, y_2) = \left(\frac{\epsilon^2(R_1-1)}{r(\epsilon+1)}, \frac{\epsilon(R_1-1)}{r(\epsilon+1)}, 0, 0 \right). \tag{7}$$

This equilibrium only has biological interpretation if $R_1 > 1$. For stability analysis, we evaluate J in Equation (5) in E_1, and yield:

$$\mathbf{J}(E_1) = \begin{bmatrix} -\frac{\epsilon(R_1-1)}{\epsilon+1} - 1 & \epsilon R_1 \left(1 - \frac{\epsilon(R_1-1)}{R_1(\epsilon+1)} - \frac{R_1-1}{R_1(\epsilon+1)}\right) - \frac{\epsilon(R_1-1)}{\epsilon+1} & 0 & -\frac{\beta\epsilon(R_1-1)}{R_1(\epsilon+1)} \\ 1 & -\epsilon & 0 & -\frac{\eta(R_1-1)}{R_1(\epsilon+1)} \\ 0 & 0 & -\gamma & s \\ 0 & 0 & \gamma & -\frac{\xi(R_1-1)}{R_1(\epsilon+1)} - \delta - u \end{bmatrix}.$$

The characteristic polynomial of $\mathbf{J}(E_1)$ is given by

$$P_3(\lambda)\ P_4(\lambda) = 0,$$

where $P_3(\lambda) = (1+\epsilon)\lambda^2 + (1+\epsilon(R_1+1)+\epsilon^2)\lambda + \epsilon(1+\epsilon)(R_1-1)$ and $P_4(\lambda) = p_{42}\lambda^2 + p_{41}\lambda + p_{40}$ with

$$\begin{aligned} p_{42} &= (1+\epsilon)R_1, \\ p_{41} &= R_1(1+\epsilon)(\gamma+\delta+u)(R_1-1), \\ p_{40} &= R_1((\delta+u)(1+\epsilon)+\xi) - R_1 s(1+\epsilon) - \xi. \end{aligned}$$

Since R_1 has already been determined from the existence condition of E_1, the equation $P_3(\lambda) = 0$ will always yield eigenvalues with negative real parts. On the other hand, $P_4(\lambda) = 0$ will have roots with negative real parts if $R^x_{\text{inv}} < 1$, where

$$R^x_{\text{inv}} = \frac{\xi + R_1 R_2(\delta+u)(1+\epsilon)}{R_1((\delta+u)(1+\epsilon)+\xi)}. \tag{8}$$

The above results is summarized in the following theorem.

Theorem 3.2. *The equilibrium point E_1 of system (4) is exist if and only if $R_1 > 1$. Furthermore, it is locally asymptotically stable if*

$$R^x_{inv} = \frac{\xi + R_1 R_2(\delta+u)(1+\epsilon)}{R_1((\delta+u)(1+\epsilon)+\xi)} < 1.$$

Otherwise, if $R^x_{inv} > 1$, the equilibrium point E_1 becomes unstable.

3.3. Extinction of *Oryzas Nigrimas*

The third equilibrium of system (4) is the equilibrium when *Oryzas Nigrimas* extinct from the ecosystem. Structurally, this equilibrium is given when $x_1 = x_2 = 0$. From direct calculation, this equilibrium is given by:

$$E_2 = (x_1, x_2, x_3, x_4) = \left(0, 0, \frac{(\delta+u)(R_2-1)}{R_2(\gamma+\delta+u)}, \frac{\gamma(R_2-1)}{R_2(\gamma+\delta+u)}\right). \tag{9}$$

It can be seen that E_2 has a biological interpretation if and only if $R_2 > 1$. For the local stability analysis, substituting E_2 into $\mathbf{J}$ gives

$$\mathbf{J}(E_2) = \begin{bmatrix} -\frac{\beta(R_2-1)\gamma}{R_2(\gamma+\delta+u)} - 1 & \epsilon R_1 & 0 & 0 \\ 1 & -\frac{\eta(R_2-1)\gamma}{R_2(\gamma+\delta+u)} - \epsilon & 0 & 0 \\ 0 & 0 & -\frac{(\delta+u)(R_2-1)\gamma}{\gamma+\delta+u} - \gamma & J_{34} \\ 0 & -\frac{\xi(R_2-1)\gamma}{R_2(\gamma+\delta+u)} & \gamma & -\delta-u \end{bmatrix},$$

where $J_{34} = (\delta+u) R_2 \left(1 - \dfrac{(\delta+u)(R_2-1)}{R_2(\gamma+\delta+u)} - \dfrac{(R_2-1)\gamma}{R_2(\gamma+\delta+u)}\right) - \dfrac{(\delta+u)(R_2-1)\gamma}{\gamma+\delta+u}$.

The characteristic polynomial of $\mathbf{J}(E_2)$ is

$$P_5(\lambda)\ P_6(\lambda) = 0,$$

where $P_5(\lambda) = (\gamma+\delta+u)\lambda^2 + (\delta\gamma R_2 + u\gamma R_2 + \delta^2 + \delta\gamma + 2u\delta + \gamma^2 + u\gamma + u^2)\lambda + \gamma(\delta+u)(\gamma+\delta+u)(R_2-1)$, and $P_6(\lambda) = p_{62}\lambda^2 + p_{61}\lambda + p_{60}$ with

$$\begin{aligned} p_{62} &= R_2^2(\gamma+\delta+u)^2, \\ p_{61} &= R_2(1+\epsilon)(\gamma+\delta+u) + (R_2-1)(\eta+\beta)\gamma, \\ p_{60} &= ((R_2-1)\eta\gamma + \epsilon R_2(\gamma+\delta+u))\left((R_2-1)\beta\gamma + R_2(\gamma+\delta+u)\right) - \epsilon(\gamma+\delta+u)R_1R_2^2. \end{aligned}$$

It can be seen that since $R_2 > 1$ has already been established from the positivity condition of E_2, the equation $P_5(\lambda) = 0$ always yields roots with negative real parts. On the other hand, $P_6(\lambda) = 0$ will have roots with negative real parts if

$$R_{\text{inv}}^y = \frac{\epsilon(\gamma+\delta+u)R_1R_2^2}{((R_2-1)\eta\gamma + \epsilon R_2(\gamma+\delta+u))\left((R_2-1)\beta\gamma + R_2(\gamma+\delta+u)\right)} < 1. \tag{10}$$

The above analytical results are summarized in the following theorem.

Theorem 3.3. *The equilibrium point E_2 of system (4) exist if $R_2 > 1$. Furthermore, it is locally asymptotically stable if*

$$R_{\textit{inv}}^y = \frac{\epsilon(\gamma+\delta+u)R_1R_2^2}{((R_2-1)\eta\gamma + \epsilon R_2(\gamma+\delta+u))\left((R_2-1)\beta\gamma + R_2(\gamma+\delta+u)\right)} < 1.$$

Otherwise, if $R_{\textit{inv}}^y > 1$, the equilibrium point E_2 becomes unstable.

3.4. Coexistence Equilibrium

The last equilibrium is the coexistence equilibrium, where *Oryzas Nigrimas* and *Nile Tilapia* coexist together in Poso Lake. This equilibrium represnted in this article as a function of y_2 due to it complex form to be written explicitely. This equilibrium is denoted by E_3 and is given by

$$E_3 = (x_1, x_2, y_1, y_2) = \left(x_1^\dagger, x_2^\dagger, y_1^\dagger, y_2^\dagger\right), \tag{11}$$

where

$$
\begin{aligned}
x_1^\dagger &= \frac{r x_2^\dagger (1 - x_2^\dagger)}{1 + r x_2^\dagger + \beta y_2^\dagger} = \frac{\Big(\gamma s (1 - y_2^\dagger) - (u+\delta)(\gamma + s y_2^\dagger)\Big)(\epsilon + \eta y_2^\dagger)}{\xi(\gamma + s y_2^\dagger)},\\
x_2^\dagger &= \frac{x_1^\dagger}{\epsilon + \eta y_2^\dagger} = \frac{\gamma s (1 - y_2^\dagger) - (u+\delta)(\gamma + s y_2^\dagger)}{\xi(\gamma + s y_2^\dagger)},\\
y_1^\dagger &= \frac{(1 - y_2^\dagger) s y_2^\dagger}{(\gamma + s y_2^\dagger)},
\end{aligned}
$$

while $y_2^\dagger$ is taken from the positive roots of the following polynomial.

$$
f(y_2) = f_3 y_2^3 + f_2 y_2^2 + f_1 y_2 + f_0 = 0, \tag{12}
$$

where

$$
\begin{aligned}
f_3 &= \beta s \eta \xi,\\
f_2 &= \xi\left(\beta(\epsilon s + \eta\gamma) + \eta s\right) - r s \eta(\gamma + \delta + u),\\
f_1 &= \beta\epsilon\gamma\xi + \eta\gamma r s + \epsilon s \xi + \eta\gamma\xi - r\left(\delta\epsilon s + \delta\eta\gamma + \epsilon\gamma s + \epsilon s u + \eta\gamma u + \delta s + \gamma s + s u + s\xi\right),\\
f_0 &= \gamma\epsilon\left[R_1(R_2 - 1)((1+\epsilon)(\delta + u)) - \epsilon(R_1 - 1)\right].
\end{aligned}
$$

The polynomial $f(y_2)$ is obtained by substituting the equilibrium expressions of the remaining variables into the equilibrium condition of y_2. Its roots therefore determine the biologically feasible coexistence equilibrium. Ecologically, $f(y_2) = 0$ represents the balance between intra and interspecific interaction between two species. Positive real roots correspond to equilibrium population levels that permit long-term coexistence. It can be seen that the expression of E_3 will always have a biological interpretation as long as $y_2^\dagger > 0$. To analyze the possible positive roots of $f(y_2)$, we apply Descartes' Rule of Signs. The results are presented in Table 1.

Table 1: Possible sign changes and corresponding positive roots of $f(\lambda)$.

Case	f_3	f_2	f_1	f_0	Sign changed	Possible positive roots
1	+	+	+	+	0	0
2	+	+	+	-	1	1
3	+	+	-	+	2	0 or 2
4	+	+	-	-	1	1
5	+	-	+	+	2	0 or 2
6	+	-	+	-	3	1 or 3
7	+	-	-	+	2	0 or 2
8	+	-	-	-	1	1

From Table 1, we can see that whenever $f_0 < 0$ (Cases 2, 4, 6, and 8), there always exists a positive root $y_2^\dagger$. From direct calculation, we obtain

$$
f_0 < 0 \Leftrightarrow R_3 = \frac{R_1(R_2 - 1)((1+\epsilon)(\delta + u))}{\epsilon(R_1 - 1)} > 1.
$$

Furthermore, it is also possible to have more than one positive root $y_2^\dagger$ (see Cases 3, 5, 6, and 7). Table 1 provides a classification of the possible number of positive roots of $f(\lambda)$ using Descartes' Rule of Signs. Ecologically, each positive root corresponds to a biologically feasible coexistence equilibrium. The condition $f_0 < 0$, equivalently $R_3 > 1$, guarantees the existence of at least one positive equilibrium, indicating that coexistence becomes possible once the threshold exceeds unity. Cases admitting more than one positive root suggest the possibility of multiple equilibrium states under different parameter regimes. This result is summarized in the following theorem.

Theorem 3.4. *The equilibrium point E_3 of system (4) exists biologically if*

$$
R_3 = \frac{R_1(R_2 - 1)(1+\epsilon)(\delta + u)}{\epsilon(R_1 - 1)} > 1.
$$

Moreover, depending on the parameter values, it is possible to have more than one positive root $y_2^\dagger$.

Since the system dimension is in four dimension, analytical eigenvalue expression are not available in closed form. Therefore, the stability of E_3 will be analyzed numerically using continuation techniques in the following numerical section.

4. Numerical Experiment

4.1. Model Parameter Estimation

Instead of directly fitting to field data from Lake Poso, the parameters of the model were established using biological information found in the literature because site-specific quantitative data for the lake are currently unavailable. This strategy aims to produce biologically plausible parameter ranges that accurately represent the life-history traits of the invasive species *Nile Tilapia* and the native species *Oryzias Nigrimas*.

- **Carrying capacity of *Oryzias Nigrimas* (K) and *Nile Tilapia* (M).** To the best of our knowledge, there is no literature that mentions the actual carrying capacity of *Nile Tilapia* or *Oryzias nigrimas*. However, we may still be able to estimate it through the following approach. According to [25], the total area of Lake Poso is approximately 39,890 ha. Furthermore, it is reported that the average yield potential of Lake Poso is 63.8 kg/ha/year. Hence, the total biomass per year is $Y_{\text{total}} = 63.8 \times 39,890 = 2,544,982$ kg/year $= 2,545$ ton/year. Based on this, the standing biomass, denoted by B, is approximated by $B \approx \lambda Y_{\text{total}}$, with $\lambda \in [0.5, 2]$. We assume $\lambda = 1$. Hence, $B = 2,545$ ton. With this value of B, we convert the biomass into the number of individuals using the formula $N \approx \frac{B}{w}$, where w represents the average weight of one fish. For a small fish such as *Oryzias nigrimas*, we assume $w = 2$ gram. Hence, the maximum carrying capacity for *Oryzias nigrimas* is $\bar{K} \approx 1,272,491,000$. On the other hand, for a medium-sized fish such as *Nile Tilapia*, we assume the average weight of each fish is 200 gram, which gives an approximate carrying capacity for *Nile Tilapia* of $\bar{M} \approx 12,724,910$. Assuming that from total area of lake Poso, only 10% of it was covered by both fish, then we have $K = 12,724,910$ and $M = 127,249$.
- **Growth rate $\bar{r}$ and $\bar{s}$.** According to [26], *Oryzias nigrimas* in Lake Poso can breed at most 5 times a year. There are no real data on the actual values of $\bar{r}$ and $\bar{s}$. Hence, we assume that $\bar{r}$ and $\bar{s}$ are between $\left[10^{-4}, 10^{-2}\right]$ day^{-1}.
- **Predation rate $\bar{\beta}$ and $\bar{\eta}$.** Similar to the growth rate, the predation rate is also difficult to find its exact value in the literature. As an assumption, we let $\bar{\beta}$ and $\bar{\eta}$ be between $[0, 10^{-7}](\text{ind} \cdot \text{day})^{-1}$.
- **Natural death rate of *Oryzias nigrimas*, $\bar{\epsilon}$.** According to [27], the average life expectancy of *Oryzias nigrimas* is around 1.67 to 3.16 years. Hence, we have $\bar{\epsilon} \in [0.000867, 0.0016]\text{day}^{-1}$.
- **Maturity rate of *Oryzias nigrimas*, $\bar{\alpha}$.** From the same reference [27], it was approximated that *Oryzias nigrimas* can be categorized as an adult after one to two years. Hence, $\bar{\alpha} \in [0.001, 0.002]\text{day}^{-1}$.
- **Natural death rate of *Nile Tilapia*, $\bar{\delta}$.** It is approximated that *Nile Tilapia* can live between 0.74 up to 3 years [28]. Hence, we have $\bar{\delta} \in [0.0009, 0.003]\text{day}^{-1}$.
- **Maturity rate of *Nile Tilapia*, $\bar{\gamma}$.** Sexual maturity of *Nile Tilapia* is reached at 3–12 months [29]. Hence, $\bar{\gamma} \in [0.002, 0.011]\text{day}^{-1}$.
- **Internal competition of *Nile Tilapia*, $\bar{\xi}$.** This parameter is also one of our model parameters for which it is difficult to find a reference value. Therefore, we assume $\bar{\xi} \in [0, 10^{-5}](\text{ind} \cdot \text{day})^{-1}$.
- **Harvesting rate of *Nile Tilapia*, $\bar{u}$.** This harvesting rate for *Nile Tilapia* depends on the needs of the human population to gain economic benefit. Therefore, we assume that the harvesting rate is between none and twice a year. Based on this assumption, we have $\bar{u} \in [0, 0.0014]\text{day}^{-1}$.

With the above parameter descriptions and their ranges of values, and using the formulas for variable and parameter nondimensionalization in the previous section, we obtain the following ranges of values for the parameters and variables in system (4).

$$\begin{aligned} &r \in [0.05, 10], \quad s \in [0.05, 10], \quad \beta \in [0, 89], \quad \eta \in [0, 89], \quad \epsilon \in [0.433, 1.6], \\ &\gamma \in [1, 11], \quad \delta \in [0.45, 3], \quad \xi \in [0, 6 \times 10^4], \quad u \in [0, 1.4], \quad x_i, y_i \in [0, 1]. \end{aligned} \tag{13}$$

4.2. Sensitivity Analysis

To investigate the relative influence of model parameters in (4) on the threshold parameters $R_1, R_2, R_3, R^x_{\text{inv}}$, and R^y_{inv}, we perform a global sensitivity analysis based on Latin Hypercube Sampling (LHS) method and combined it with Partial Rank Correlation Coefficient (PRCC). The expression of the above threshold are a nonlinear function of multiple biological parameters, and hence their analytical dependence is highly nontrivial. Furthermore, we mentioned in the previous section that some of our parameters are difficult to estimated due to the lack of references. Hence, sensitivity analysis can fill this gap. We use 5000 samples from our range of parameter values from previous section, and show it as a sensitivity diagram in Figure 1 and 2.

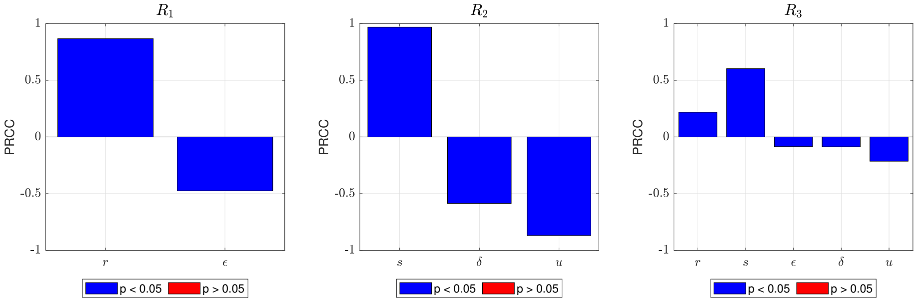

Figure 1: PRCC results for R_1, R_2, and R_3.

From Figure 1, it can be seen that all parameters in R_1, R_2, and R_3 are significant in determining the value of the respective thresholds. In R_1 and R_2, we can see that the growth rates r and s are the most significant parameters with positive PRCC values, which indicates that increasing these parameters will increase R_1 and R_2, respectively. On the other hand, the natural death rates ϵ and δ, and human intervention through harvesting, have negative PRCC values. For R_3, the results show that the growth rate of *Nile Tilapia*, denoted by s, is the most significant parameter in determining R_3. This result indicates that increasing the growth rate of *Nile Tilapia* will increase the chance of a coexistence situation in the field. On the other hand, the harvesting rate also shows a significant role, but in a vice versa manner. Increasing the harvesting rate will decrease the chance of a coexistence situation in the ecosystem.

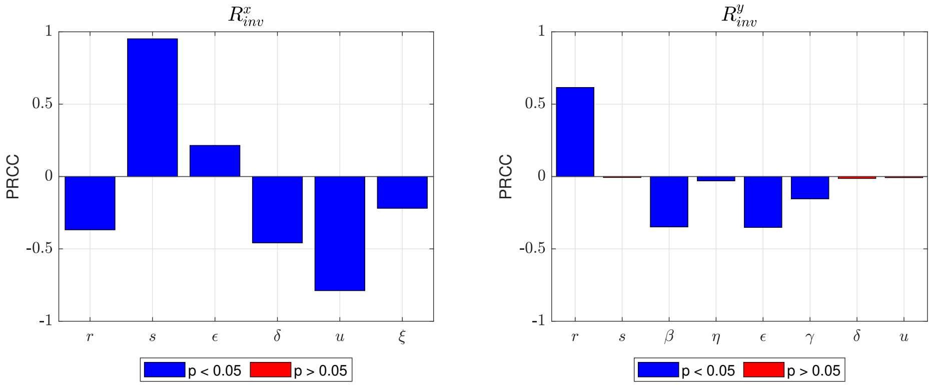

Figure 2: PRCC results for R^x_{inv}, and R^y_{inv}. The red bars represent insignificant parameters for the related threshold since $p_{\text{value}} > 0.05$.

For the invasion thresholds R^x_{inv} and R^y_{inv}, the PRCC results are depicted in Figure 2. We can see that R^x_{inv} is very sensitive to the growth rate of *Nile Tilapia* and its harvesting rate. Previously, we have shown that *Oryzias nigrimas* will exist alone in the population if $R^x_{\text{inv}} < 1$. Therefore, in order to achieve this situation, one option is to reduce s or increase u. On the other hand, R^y_{inv} is significantly sensitive to the growth rate, competition coefficient, and natural death rate of *Oryzias nigrimas*. These results indicate that when the local fish, which in this case is *Oryzias nigrimas*, is weak in competing with the invasive fish, or when its natural death rate is very high, then the extinction of the local fish becomes very possible. Hence, controlling external factors such as regulated harvesting is very crucial in achieving coexistence between these two fish. We will perform this controlled harvesting in the next section.

4.3. Bifurcation Diagram

In this section, we conduct a continuation approach to obtain the bifurcation diagram. We use *MatCont* to perform the simulation. *MatCont* is a continuation software that runs on MATLAB and can be used to carry out continuation experiments. To perform the simulation, we first need to determine all possible equilibrium points that arise from the chosen parameter values. Using the following parameter set:

$$r = 2.5, \beta = 0.3, \epsilon = 0.8, \eta = 0.2, s = 2, \gamma = 1.2, \delta = 0.5, \xi = 0.2, u = 1,$$

we obtain $R_1 = 3.125$, $R_2 = 1.33$, $R^x_{\text{inv}} = 1.25$, $R^y_{\text{inv}} = 1.089$, and $R_3 = 1.654$. With these parameter values, we find all possible equilibrium points as follows:

$$E_0 = (0, 0, 0, 0),\ E_1 \quad = (0.302, 0.377, 0, 0),\ E_2 = (0, 0, 0.138, 0.111),\ E_3 \quad = (0.298, 0.364, 0.121, 0.092),$$

where only E_3 is a stable equilibrium point, while the others are unstable. Next, we choose u as the bifurcation parameter to investigate the impact of harvesting on the *Nile Tilapia* population. The results are depicted in Figure 3.

The interpretation of Figure 3 is as follows. We use the harvesting rate of *Nile Tilapia* as the bifurcation parameter, allowing it to vary continuously along the x-axis from $u = 0$ up to $u = 2$. Note that from the expressions of R_1, R_2, R^x_{inv}, and R^y_{inv} in the previous section, the parameter u appears in all of these thresholds except R_1. Therefore, the population of *Oryzas Nigrimas* always exists for all values of u (see panels (a) and (b)), whether from E_1 or E_3. Furthermore, we can also see that E_0 is always unstable, represented by the red curve along the x-axis. For small values of u, starting from $u = 0$ and increasing gradually, we observe that E_1 and E_2 exist but remain unstable. As mentioned earlier, u does not affect the value of R_1, hence x_1 and x_2 remain constant for all values of u, i.e., $E_1 = (0.302, 0.377, 0, 0)$. At the same time, x_1 and x_2 in E_3 increase as u increases, indicating that harvesting *Nile Tilapia* promotes the growth of *Oryzas Nigrimas*. Conversely, as u increases, the *Nile Tilapia* population generally decreases, except for the juvenile class y_1, which initially increases and then decreases as u becomes larger. It can be seen that E_3 remains stable for all u until it reaches the branching point BP1 at $u = 1.424$. Beyond this point, the stability of E_3 changes from stable to unstable, and simultaneously, E_1 becomes stable. Moreover, for $u >$ BP1, E_3 not only loses stability but also disappears, as y_1 and y_2 on this branch become negative. From panels (c) and (d), we observe that E_2 exists for all $u <$ BP2, where BP2 corresponds to $u = 1.5$ such that $R_2 = 1$. Although E_2 exists, it remains unstable since for all $u <$ BP2, $\mathcal{R}^y_{\text{inv}}$ is always greater than one. The equilibrium E_2 disappears when u surpasses BP2.

To visualize the impact of u on the dynamic of system (4), we solve system (4) with ODE45 toolbox in *MatLab* using same parameter values as before, and initial condition $(0.2, 0.1, 0.2, 0.05)$. The results depicted in Figure 4. From this simulation, we can clearly see the importance of controlled harvesting of *Nile Tilapia* to ensure the coexistence between *Oryzas Nigrimas* and *Nile Tilapia* within the Lake Poso ecosystem.

4.4. Effect of Invasion on Juvenile *Oryzas Nigrimas*

For the next simulation, we numerically examine the impact of the invasion of *Nile Tilapia* on juvenile *Oryzas nigrimas* by varying the values of β. The same parameter values as in the previous simulation are used, except that β is varied as $0.3, 1.3, 2.3, 3.3$, and 4.3. The results are shown in Figure 5. It can be clearly observed that as the invasion intensity increases, the population of juvenile *Oryzas nigrimas* decreases significantly. Consequently, the population of adult *Oryzas nigrimas* also declines due to the reduced recruitment from the juvenile stage. In contrast, the impact of this massive invasion only slightly affects the population of *Nile*

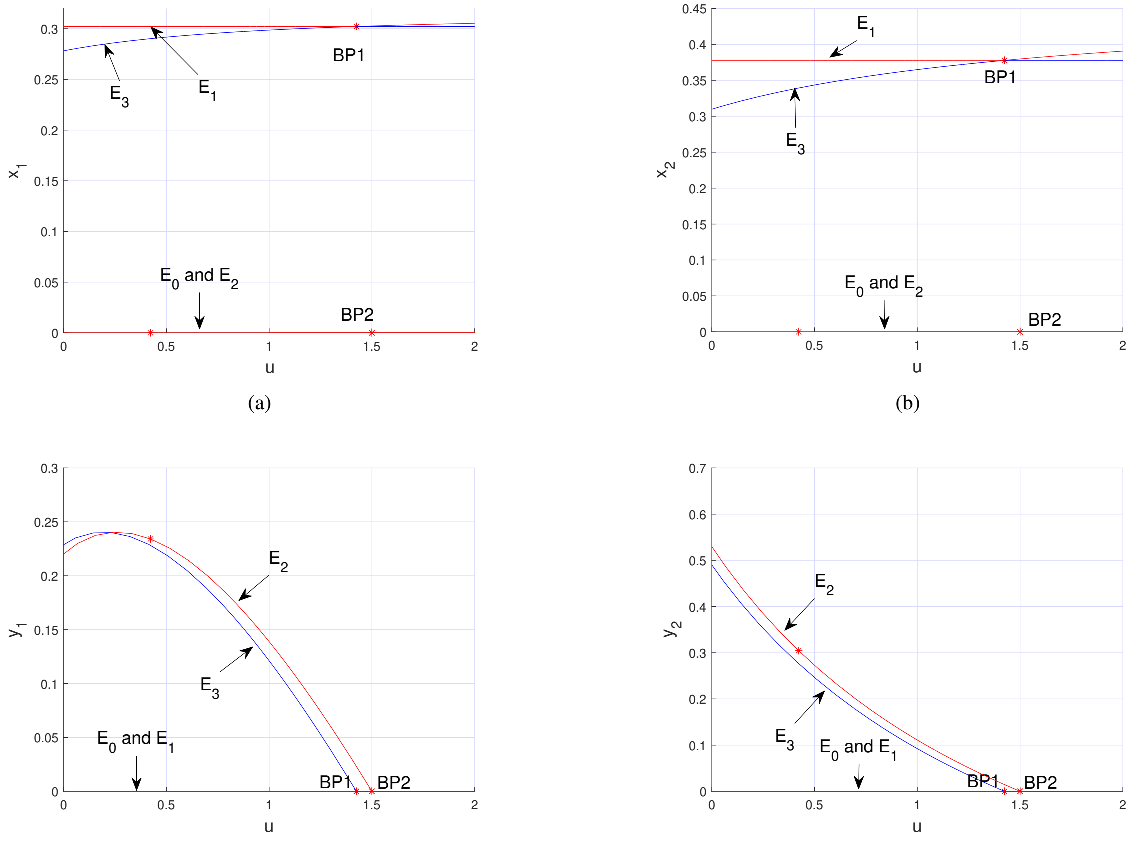

(a) (b)

(c) (d)

Figure 3: Bifurcation diagram of x_1, x_2, y_1, and y_2 from panel (a) to (d), respectively using u as the bifurcation parameter. Red and blue curves represent unstable and stable equilibrium points, respectively. Furthermore, BP1 and BP2 represent value of u such that R^x_{inv} and R_2 equals to one, respectively.

Tilapia. It is evident that as the invasion pressure on juvenile *Oryzas nigrimas* becomes more intense, the population of *Nile Tilapia* increases, since the interspecific competition between the two species is weakened.

4.5. Effect of periodic harvest on *Nile Tilapia*

Let us define the periodic harvesting $u(t)$ as follows:

$$u(t) = u_c\, H\big((t \bmod T) - cT\big), \qquad t \in [0,\, 5T],$$

where $H(x)$ is the heaviside function defined as

$$H(x) = \begin{cases} 0, & x < 0, \\ 1, & x \geq 0, \end{cases}$$

and $c \in (0, 1)$. The interpretation of u_c, c, and T is as follows:

- u_c is the harvest intensity applied during the active phase of the cycle. Mathematically, it scales how fast the population (e.g., prey, fish, or resource species) is removed during harvesting. A higher u_c

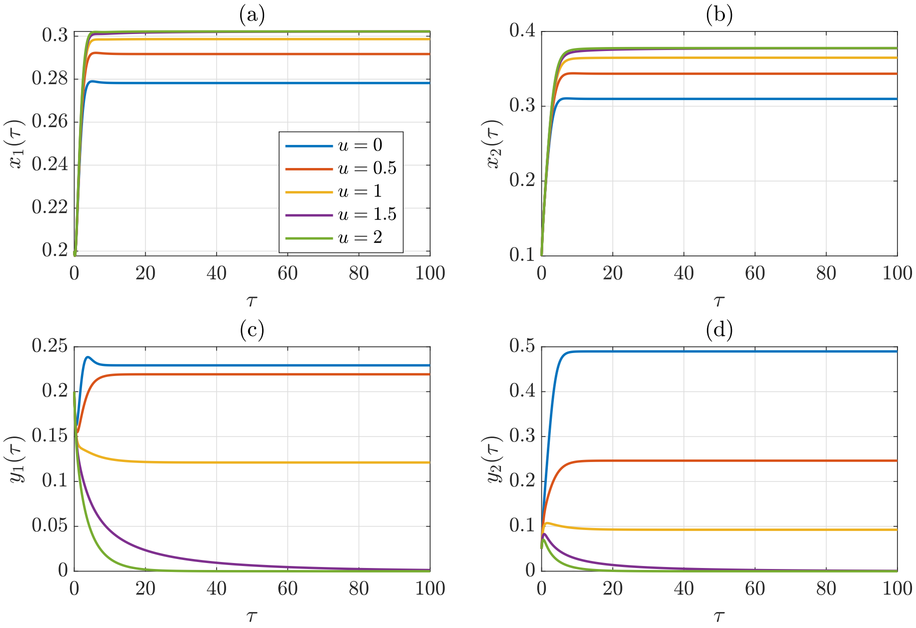

Figure 4: Dynamic of x_1, x_2, y_1, and y_2 respect to variation of u in panel (a) to (d), respectively.

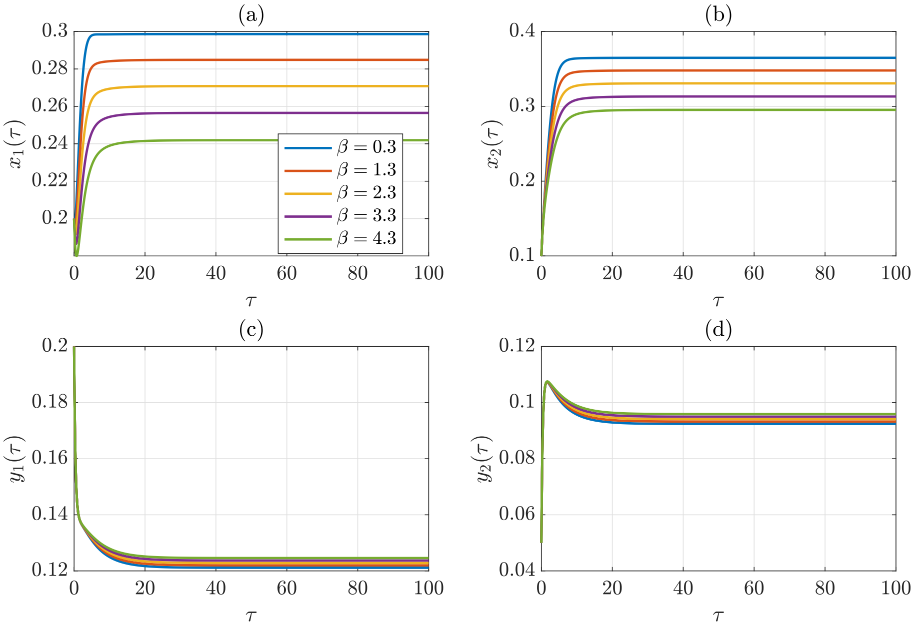

Figure 5: Dynamic of x_1, x_2, y_1, and y_2 respect to variation of β in panel (a) to (d), respectively.

means stronger or more aggressive harvesting, which can rapidly reduce population size but might risk depletion.
- $c \in (0, T)$ defines the fraction of each period T after which harvesting begins. c controls when and for how long harvesting occurs within each cycle. It effectively tunes the harvest duty cycle — the balance between rest (no harvesting) and active removal.
- T represent the duration of one harvesting cycle period. Small T implies frequent harvests, while larger T means longer recovery intervals for the population.

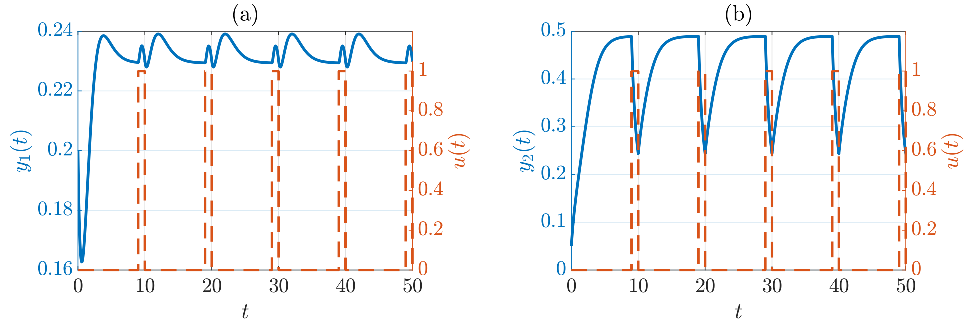

Figure 6: Impact of $u(t)$ with one specific sample $u_c = 1$ on the dynamic of y_1 and y_2 for panel (a) and (b), respectively. Red and blue curve represent the time varying $u(t)$ and dynamic of *Nile Tilapia*, respectively.

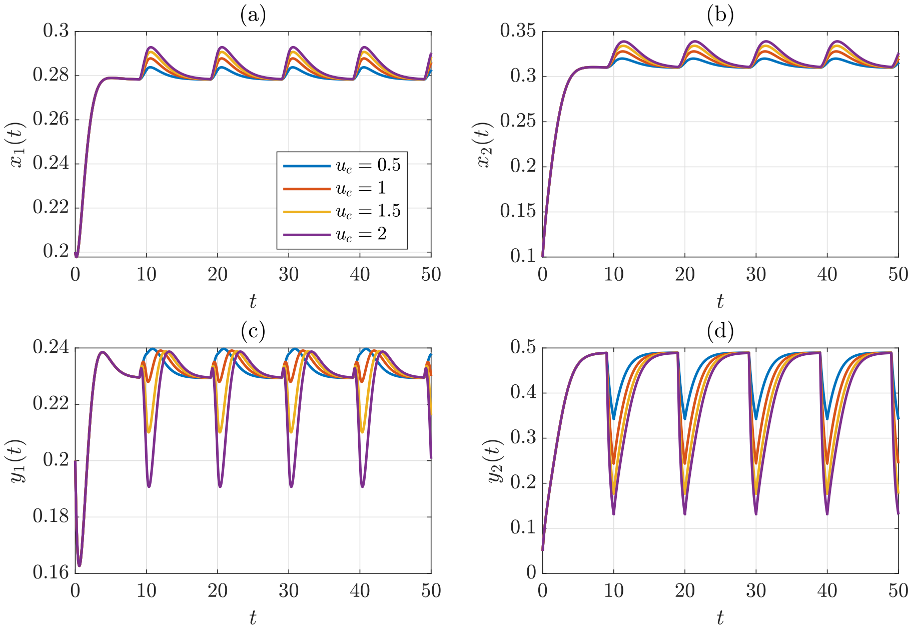

Figure 7: Impact of $u(t)$ under the variation of u_c on the dynamic of system (4).

The first numerical experiment using $u(t)$ is conducted by varying u_c, while keeping $c = 0.9$ and $T = 10$ fixed. The values of u_c are chosen as $0.5, 1, 1.5$, and 2 to represent different levels of harvesting intensity during the active harvesting phase, $t \in [0.9T, T]$. For $u_c = 1$, the results are presented in Figure 6, which illustrates the impact of harvesting on the dynamics of y_1 and y_2. Since $u(t)$ is applied only to harvest adult *Nile Tilapia*, the population of adults (y_2) decreases significantly during the harvesting interval and then recovers to its natural equilibrium once harvesting ceases. In contrast, the juvenile population (y_1) increases temporarily during this period due to the reduction in adult density. From a biological perspective, this transient growth of y_1 reflects a *buffer effect* or *compensatory accumulation* within the immature or non-harvested subpopulation. When mature individuals are removed, the overall environmental pressure and density-dependent limitation are temporarily alleviated, allowing the immature class to accumulate before gradually declining as maturation and subsequent harvesting resume in the next cycle.

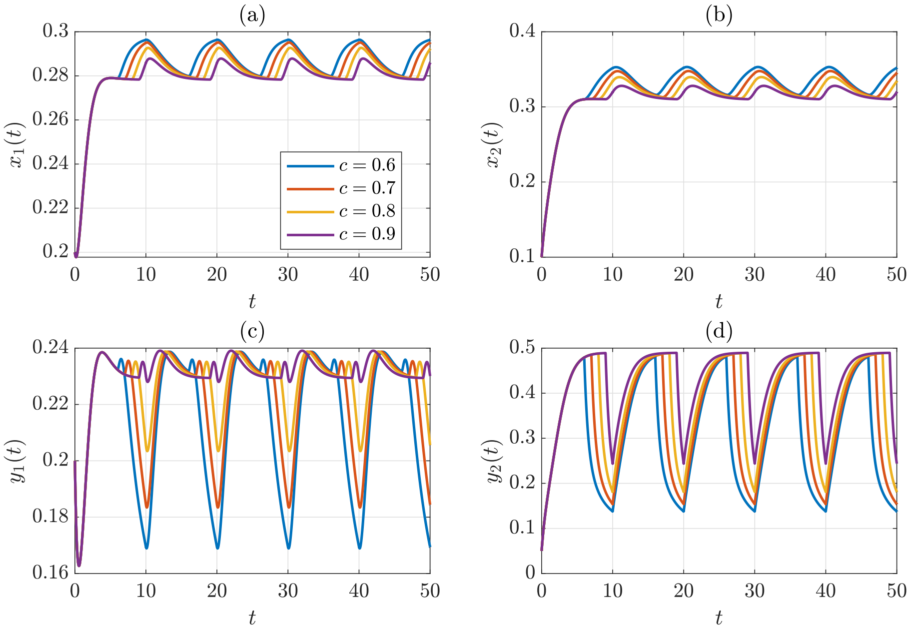

Figure 8: Impact of $u(t)$ under the variation of c on the dynamic of system (4).

The results for varying u_c are shown in Figure 7. As noted earlier, y_2 naturally declines substantially during the harvesting phase and recovers once the harvesting period ends. Larger values of u_c result in a more pronounced reduction in y_2 and require a longer time for recovery. A similar pattern is also observed in the juvenile population. On the other hand, harvesting does not directly affect the population of *Oryzas Nigrimas*. Nevertheless, an indirect effect emerges: as the harvesting intensity of adult *Nile Tilapia* increases, the population of *Oryzas Nigrimas* tends to rise, benefiting from reduced competition or predation pressure.

The next simulation is presented in Figure 8, where we investigate the effect of varying the duration of the harvesting period, denoted by c in $u(t)$, while we fix $u_c = 1$ and $T = 10$. A smaller value of c corresponds to a longer harvesting duration. In this experiment, we consider $c = 0.6, 0.7, 0.8,$ and 0.9. It can be observed that extending the harvesting window exerts a more pronounced impact on the populations of *Oryzas nigrimas* and *Nile Tilapia*. When the harvesting duration becomes longer, the population of *Nile Tilapia* declines more substantially and requires a longer time to recover to its natural dynamic state. Consequently, the population becomes more vulnerable during extended harvesting periods. On the other hand, the population of *Oryzas nigrimas* benefits from the reduction in *Nile Tilapia*, as interspecific competition is weakened. As a result, the population of *Oryzas nigrimas* tends to increase as the harvesting window for *Nile Tilapia* becomes wider.

5. CONCLUSIONS

Here in this article, we have introduced a novel mathematical model describing the interaction between *Nile Tilapia* and *Oryzias nigrimas* in Lake Poso. The model is analyzed both analytically and numerically. From our analytical results, we identify four different equilibrium points, namely the extinction of all species, the existence of only one species, and the coexistence equilibrium points where *Nile Tilapia* and *Oryzias nigrimas* can coexist even when harvesting on *Nile Tilapia* is applied. We found five different thresholds that play an important role in determining the existence and stability of each equilibrium point, namely the local offspring numbers (R_1 and R_2), the invasion reproduction numbers (R_{inv}^x and R_{inv}^y), and a combined threshold derived from the local offspring numbers. Analytically, we found that for each species to persist, its corresponding local offspring number must be greater than one. To dominate the other species, its specific invasion number must also exceed one. These results are visualized through a bifurcation diagram obtained using the continuation method implemented in *MatCont*. To analyze the impact of periodic harvesting, we introduce a harvesting rate modeled as an impulse function, where the intensity, timing, and duration of harvesting act as control parameters. This function is defined using a Heaviside representation. Numerical results reveal that the intensity of harvesting plays a crucial role in maintaining the coexistence of *Nile Tilapia* and *Oryzias nigrimas* in Lake Poso. The longer or more intense the harvesting applied, the longer the recovery time required for the ecosystem to return to balance.

ACKNOWLEDGEMENT

This research was supported by the Ministry of Education, Culture, Research, and Technology of the Republic of Indonesia, Directorate General of Higher Education, Research, and Technology. (ID number: PKS-470/UN2.RST/HKP.05.00/2025).

REFERENCES

[1] Herjayanto, M., Gani, A., Adel, Y.S. and Suhendra, N., Frehswater fish of lakes and it's inlet rivers in Sulawesi Tengah Province, Indonesia, Journal of Aquatropica Asia, 4(1), pp. 1–9, 2019.

[2] Serdiati, N., Arfiati, D., Widodo, M.S., Lelono, T.J., Ndobe, S. and Saranga, R., Morphological variations and phylogenetic analysis of Oryzias nigrimas kottelat, 1990 (rice fish) from Lake Poso, Central Sulawesi, Indonesia, Biodiversitas Journal of Biological Diversity, 21(3), 2020.

[3] Takehana, Y., Naruse, K. and Sakaizumi, M., Molecular phylogeny of the medaka fishes genus Oryzias (Beloniformes: Adrianichthyidae) based on nuclear and mitochondrial DNA sequences, Molecular Phylogenetics and Evolution, 36(2), pp. 417–428, 2005.

[4] Martin, C.W., Valentine, M.M. and Valentine, J.F., Competitive interactions between invasive Nile tilapia and native fish: the potential for altered trophic exchange and modification of food webs, PloS One, 5(12), p. e14395, 2010.

[5] Rao, W., Ning, J., Zhong, P., Jeppesen, E. and Liu, Z., Size-dependent feeding of omnivorous Nile tilapia in a macrophyte-dominated lake: implications for lake management, Hydrobiologia, 749(1), pp. 125–134, 2015.

[6] Luis, P., Kamalia, P.Z., Peter, O.J. and Aldila, D., Implementation of non-standard finite difference on a predator-prey model considering cannibalism on predator and harvesting on prey, Jambura Journal of Biomathematics, 6(1), pp. 35–43, 2025.

[7] Suandi, D., Ansori, M.F., Aldila, D., Noviantri, V., Sobari, E. and Nasir, N.B.M., Investigating the efficacy of insecticides in controlling the spread of tungro virus in rice plants: a mathematical modelling approach, Communications in Mathematical Biology and Neuroscience, 2025, Article 59, 2025.

[8] Suandi, D., Aldila, D., Noviantri, V., Sobari, E. and Nasir, N.B.M., Mathematical modelling that characterizes the qualitative behavior of the interactions of aphids and ladybugs as insectivorous animals, Communications in Mathematical Biology and Neuroscience, 2023, Article 106, 2023.

[9] Aldila, D. and Windyhani, T., Backward bifurcation emerging from a mathematical model of African animal trypanosomiasis disease in white rhino populations, Journal of Mathematical and Fundamental Sciences, 54(1), pp. 151–189, 2022.

[10] Wijaya, K.P., Páez Chávez, J., Pochampalli, R., Rockenfeller, R., Aldila, D., Götz, T. and Soewono, E., Food sharing and time budgeting in predator-prey interaction, Communications in Nonlinear Science and Numerical Simulation, 97, p. 105757, 2021.

[11] Tabornal, R.U., Escaner IV, J.M.L. and Rabajante, J.F., Mathematical modeling on competition and cooperation of species using Hill-type function, *Proceedings of the 11th International Conference on Computer Modeling and Simulation*, pp. 8–18, 2019.

[12] Gutnik, D.I., Belykh, T.I., Rodionov, A.V. and Bukin, Y.S., Mathematical model of competition for a limited resource in ecosystems: numerical and analytical study of sustainability, Modeling, Optimization and Information Technology, 13(2), pp. 51–76, 2025.

[13] Lu, N., Liu, C. and Guo, J., Dynamical analysis in an exploited two-species competition model with double time delays, *2016 Chinese Control and Decision Conference (CCDC)*, pp. 2073–2078, 2016.

[14] Shukla, J., Agrawal, A., Dubey, B. and Sinha, P., Existence and survival of two competing species in a polluted environment: a mathematical model, Journal of Biological Systems, 9(02), pp. 89–103, 2001.

[15] James Omaiye, O., Numerical analysis of ordinary differential equations of ecological competing species across diverse environments, African Journal of Mathemafics and Stafisfics Studies, 6(1), pp. 88–102, 2023.

[16] Chen, S., Chen, F., Srivastava, V. and Parshad, R.D., Dynamical analysis of an allelopathic phytoplankton model with fear effect, Qualitative Theory of Dynamical Systems, 23(4), p. 189, 2024.

[17] Chen, S., Chen, F., Srivastava, V. and Parshad, R.D., Dynamical analysis of a lotka–volterra competition model with both allee and fear effects, International Journal of Biomathematics, 17(08), p. 2350077, 2024.

[18] Hu, J., Liu, J., Yuen, P.W., Li, F. and Deng, L., Modelling of a seasonally perturbed competitive three species impulsive system, AIMS Press, 2022.

[19] Lou, Y., Tao, W. and Wang, Z.-A., Effects and biological consequences of the predator-mediated apparent competition II: PDE models, Journal of Mathematical Biology, 91(5), p. 55, 2025.

[20] Leticia, O. and Oleka, L., Mathematical model for the dynamic behavior of two competing plant species, International Journal of Scientific and Research publications, 6(5), pp. 498–502, 2016.

[21] Novalina, S., Diana, A., Sri, W.M., Djoko, L.T. and Jaya, G.B.A., Food habits of the endemic ricefishes (Oryzias nigrimas, kottelat 1990) in Poso Lake, Central Sulawesi of Indonesia, Russian Journal of Agricultural and Socio-Economic Sciences, 87(3), pp. 125–130, 2019.

[22] Sanches, F.H.C., Miyai, C.A., Costa, T.M., Christofoletti, R.A., Volpato, G.L. and Barreto, R.E., Aggressiveness overcomes body-size effects in fights staged between invasive and native fish species with overlapping niches, PLoS One, 7(1), p. e29746, 2012.

[23] Alqahtani, Z., Almuneef, A. and El-Shahed, M., Mathematical model for the control of red palm weevil, Axioms, 13(9), p. 637, 2024.

[24] Rayungsari, M., Suryanto, A., Kusumawinahyu, W.M. and Darti, I., Dynamical analysis of a predator-prey model incorporating predator cannibalism and refuge, Axioms, 11(3), p. 116, 2022.

[25] Kaban, S., Ditya, Y.C., Makmur, S., Fatah, K., Wulandari, T.N.M., Dwirastina, M., Makri, M. and Samuel, S., Water quality and trophic status to estimate fish production potential for sustainable fisheries in Lake Poso, Central Sulawesi, Polish Journal of Environmental Studies, 32(5), pp. 4083–4093, 2023.

[26] Serdiati, N., Karakterisasi ikan padi Oryzias nigrimas (kottelat, 1990) sebagai upaya pengelolaan ikan endemik di Danau Poso Sulawesi Tengah, Universitas Brawijaya, Doctoral Dissertation, Malang, Indonesia, 2019.

[27] Serdiati, N., Nurdin, M.S., Hasan, V., Mokodongan, D.F. and Safir, M., Population dynamic of endemic ricefish in Lake Poso: implications for conservation, International Journal of Conservation Science, 14(1), pp. 301–314, 2023.

[28] Ouédraogo, R.B., Sanogo, S. and Compaoré, I., Population dynamics of Nile tilapia, Oreochromis niloticus (Linnaeus, 1758) in Samendéni reservoir, Burkina Faso, Fisheries and Aquatic Sciences, 28(5), pp. 285–297, 2025.

[29] Froese, R. and Pauly, D., Oreochromis niloticus (Linnaeus, 1758), 2025. https://www.fishbase.se/summary/oreochromis-niloticus.html, Accessed on February, 2026.